Arch. Pharm. Res. (2017) 40:933–942
DOI 10.1007/s12272-017-0932-z

Online ISSN 1976-3786
Print ISSN 0253-6269

Archives of Pharmacal Research
www.springer.com/12272

RESEARCH ARTICLE

RANKL-induced osteoclastogenesis is suppressed by 4-*O*-methylhonokiol in bone marrow-derived macrophages

Kyung-Ran Park[1] · Ji-Youn Kim[2] · Eun-Cheol Kim[3] · Hyung-Mun Yun[3] · Jin Tae Hong[4]

Received: 8 April 2017 / Accepted: 17 July 2017 / Published online: 24 July 2017

Abstract Magnolol, honokiol, and obovatol are well known bioactive constituents of the bark of *Magnolia officinalis* and have been reported to have beneficial effects in various diseases. We recently isolated a novel active compound, 4-*O*-methylhonokiol (4-*O*-MH) from the ethanol extract of *M. officinalis*, which was previously reported to have pharmacological effects including anti-inflammatory, anti-oxidative, and anti-aging activities. Here, we examined the pharmacological properties of 4-*O*-MH on osteoblast (bone-forming cells) and osteoclast (bone-resorbing cells) differentiation, and its underlying signaling pathways in primary cultured pre-osteoblasts and bone marrow macrophages. Our results showed that 4-*O*-MH did not affect cell viability in pre-osteoblasts and did not influence osteoblast differentiation and mineralized nodule formation, as assessed by alkaline phosphatase activity and Alizarin red staining. However, 4-*O*-MH significantly inhibited TRAP-positive multinuclear osteoclasts and F-actin ring formation during Receptor activator of NF-κB ligand (RANKL)-mediated osteoclastogenesis without cytotoxicity. In addition, 4-*O*-MH suppressed RANKL-induced critical factors (c-Fos, NF-ATc1, TRAP, and ITB3) for osteoclast differentiation and function. Furthermore, RANKL-mediated signaling, including ERK1/2, AKT, and NF-kB pathways was attenuated by 4-*O*-MH. Taken together, 4-*O*-MH has an inhibitory role in RANKL-mediated osteoclastogenesis but not osteoblast differentiation, and our findings also suggest that 4-*O*-MH is a potential therapeutic agent for bone-destructive diseases such as osteoporosis, alveolar bone resorption, and osteoarthritis.

Keywords *Magnolia officinalis* · 4-*O*-methylhonokiol · Osteoblast · Osteoclast · RANKL

✉ Hyung-Mun Yun
yunhm@khu.ac.kr

✉ Jin Tae Hong
jinthong@chungbuk.ac.kr

[1] Department of Oral & Maxillofacial Regeneration, Graduate School, Kyung Hee University, Seoul 130-701, Republic of Korea

[2] Department of Dental Hygiene, College of Health Science, Gachon University, Incheon 406-799, Republic of Korea

[3] Department of Oral and Maxillofacial Pathology, School of Dentistry, Kyung Hee University, 1 Heogi-Dong, Dongdaemun-Gu, Seoul 130-701, Republic of Korea

[4] College of Pharmacy and Medical Research Center, Chungbuk National University, 194-31, Osongsangmyeong1-ro, Heungdeok-gu, Cheongju, Chungbuk 361-763, Republic of Korea

Introduction

Bone metabolism is a physiological process that maintains the skeleton by removing and replacing old bone (Marie and Kassem 2011). Impaired osteoblast differentiation results in poor bone quality and osteopenia (Filvaroff et al. 1999; Zanotti and Canalis 2015), and dysregulation of osteoclast differentiation results in osteoporosis which is one of the biggest challenges faced by modern medicine (Khosla and Riggs 2005; Vondracek et al. 2008).

Anti-catabolic drugs including bisphosphonates, Receptor activator of NF-κB ligand (RANKL) inhibitors, and anti-resorptives have beneficial effects on increasing bone mass in bone diseases (Riggs and Parfitt 2005). However, their ability to repair or recover bone mass has only modest effects (Riggs and Hartmann 2003). Therefore, novel and effective therapeutics for bone disease need to be identified and their effect on bone pathophysiology

studied for osteoclast-mediated bone resorption, osteoblast-mediated bone formation, and intracellular signaling pathways (Endo and Matsumoto 2012; Cairoli et al. 2015).

Traditional Chinese medicines or natural products are potential drug candidates to prevent and treat bone disease (Lee et al. 2011c; Yun et al. 2014). Previously, our group demonstrated that 2,4,5-trimethoxyldalbergiquinol isolated from *Dalbergia odorifera* which is used as a traditional herbal medicine potentiates osteoblast differentiation and mineralized nodule formation through the BMP and Wnt/β-catenin pathways (Yun et al. 2015). We recently isolated a novel neolignan compound 4-*O*-methylhonokiol (4-*O*-MH) from *Magnolia officinalis*, and demonstrated its pharmacological effects such as anti-inflammatory, anti-oxidative, anti-cancer, and anti-aging activities (Oh et al. 2009; Lee et al. 2011b, 2012; Oh et al. 2012; Jung et al. 2014). Although we studied 4-*O*-MH as a promising drug candidate under a variety of pathophysiological conditions, the pharmacological properties and mechanism of action on bone metabolism have not yet been established. Therefore, we investigated the potential effects and underlying signaling pathways of 4-*O*-MH on an in vitro cell system using primary mouse calvarial pre-osteoblasts and bone marrow macrophages (BMMs).

Materials and methods

Isolation and identification of 4-*O*-methylhonokiol from the bark of *Magnolia officinalis*

The bark of *M. officinalis* was dried in the shade at room temperature and stored in a dark, cold room until use. The air-dried bark of *M. officinalis* (3 kg) was cut into pieces and extracted twice with 95% (v/v) ethanol (four times the weight of the dried plants) for 3 days at room temperature. After filtration through 400-mesh filter cloth, the filtrate was re-filtered through filter paper (Whatman, no. 5) and concentrated under reduced pressure. The extract (450 g) was then suspended in distilled water, and the aqueous suspension was extracted with *n*-hexane, ethyl acetate, and n-butanol, respectively. The *n*-hexane layer was evaporated to dryness to give a residue (70 g), which was chromatographed on silica gel with *n*-hexane: ethyl acetate (9:1) to yield a crude fraction that included 4-*O*-methylhonokiol. This fraction was repeatedly purified by silica gel chromatography using *n*-hexane: ethyl acetate as the eluent to obtain pure 4-*O*-methylhonokiol (4-*O*-MH). The purity was greater than 99.5%. 4-*O*-methylhonokiol was identified by ^{1}H-NMR (400 MHz, $CDCl_3$): d 3.36 (2H, d, J = 7 Hz, H-7), 3.44 (2H, d, J = 7′ Hz, 70-H), 3.89 (3H, s, OMe), 5.05–5.14 (5H, m, H-9, H-9′, OH), 5.93–6.07 (2H, m, H-8, H-8′), 6.92 (1H, d, J = 7 Hz, Ar–H), 6.97 (1H, d, J = 8 Hz, Ar–H), 7.04–7.08 (2H, m, Ar–H), 7.24–7.31 (2H, m, Ar–H). ^{13}C-NMR (100 MHz, $CDCl_3$): d 34.5 (C-7), 39.6 (C-7′), 55.8 (OMe), 111.2 (C-3′), 115.7 (C-4′), 115.8 (C-9), 116.1 (C-9′), 128.0 (C-1′), 128.1 (C-6), 129.0 (C-3), 129.2 (C-1), 130.0 (C-5), 130.4 (C-6′), 130.7 (C-2), 132.4 (C-5′), 136.7 (C-8), 138.0 (C-8′), 151.0 (C-2′), 157.2 (C-4). The ethanol extract of *M. officinalis* contained 16.6% 4-*O*-MH, 16.5% honokiol and 12.9% magnolol, and 54% others.

Primary culture of mouse calvarial osteoblasts

Primary osteoblasts were isolated from calvariae of 1-day-old ICR mice after dissected aseptically and treated with 0.2% collagenase-dispase enzyme solution (Sigma-Aldrich, St. Louis, MO). Cells (passage 0) were collected by centrifuge after repeated digestions and cultured in α-minimum essential medium (α-MEM) (Gibco Laboratories, Grand Island, NY) without L-ascorbic acid supplemented with 10% fetal bovine serum (FBS), penicillin (100 units/mL), and streptomycin (100 μg/mL) at 37 °C in a humidified atmosphere of 5% CO_2 and 95% air. The cells were detached and reseeded at approximately 70–80% confluence, and then the cells (passage 1) were used for the experiments reported here. Osteoblast differentiation was induced by changing osteogenic supplement medium (OS) containing 50 μg/mL L-ascorbic acid and 10 mM β-glycerophosphate when the cells are approximately 90% confluent. The medium was replaced every 2 days during the incubation period. 4-*O*-MH was dissolved in 100% DMSO and then diluted (1: 1000) directly into the medium. A final concentration of 0.1% DMSO was used as the vehicle control.

Primary culture of bone marrow macrophages and osteoclast differentiation

Mouse bone marrow cells isolated by flushing the marrow space of femur and tibia in 5 week-old mice were incubated overnight on culture dishes in α-MEM (Gibco Laboratories) containing 10% FBS (Gibco Laboratories) and antibiotics (100 units/mL penicillin G and 100 μg/mL streptomycin) at 37 °C in a humidified atmosphere of 5% CO_2 and 95% air. After discarding adherent cells, floating cells were further incubated with mouse M-CSF (30 ng/mL) on Petri dishes. BMMs became adherent after 3 days in culture and then cells were differentiated into osteoclasts using mouse RANKL (100 ng/mL) and M-CSF (30 ng/mL) for 5 days.

MTT assay

Cell toxicity was measured by a 3-[4,5-dimethylthiazol-2-yl]-2,5-diphenyltetrazolium bromide (MTT) assay to detect NADH-dependent dehydrogenase activity. Fifty microliters

of MTT solution (5 mg/mL) in 1X phosphate-buffered saline (PBS) was directly added to the cells, which was then incubated for 2 h to allow MTT to metabolize to formazan. Absorbance was measured at a wavelength of 540 nm using an enzyme linked immunosorbent assay (ELISA) reader (Beckman Coulter, Fullerton, CA).

Alkaline phosphatase (ALP) activity

ALP activity was measured by spectrophotometry. Cells were homogenized in 0.5 mL distilled water with a sonicator, and centrifuged. The aliquots of cell homogenate were incubated with 15 mM *p*-NPP in 0.1 M glycine–NaOH (pH 10.3) at 37 °C for 30 min. The reaction was stopped by adding 0.25 N NaOH. The absorbance was measured at 405 nm using an ELISA reader (Beckman Coulter).

Alizarin red S staining

After 14 days of culture, cells were fixed in 70% ice-cold ethanol for 1 h and rinsed with distilled water. Cells were stained with 40 mM Alizarin Red S (pH 4.2) for 10 min with gentle agitation. The level of Alizarin Red S staining was observed under light microscopy. Stains were eluted with 100% DMSO to quantify the amount of alizarin red staining and measured at 590 nm.

Tartrate-resistant acid phosphatase (TRAP) staining

After BMMs were differentiated into osteoclasts for 5 days, the cells were fixed with 4% formaldehyde for 15 min. Cells were washed, and then stained for TRAP using a leukocyte acid phosphatase cytochemistry kit (Sigma) according to the manufacturer′s instructions. The TRAP-positive multinucleated cells (MNCs) containing three or more nuclei were counted as mature osteoclasts using a light microscope. Typically, cells were mostly TRAP-positive and mononuclear at 2 days after induction with RANKL and TRAP-positive and multinuclear 2 or 3 days later. We considered mononuclear TRAP-positive cells to be preosteoclasts and multinuclear TRAP-positive cells to be mature osteoclasts as described previously (Chang et al. 2008).

Actin-ring formation analysis

Osteoclasts were fixed with 4% formaldehyde, permeabilized with 0.1% Triton X-100, and incubated with FITC-phalloidin (Invitrogen) for 30 min. After being washed with PBS, the cells were incubated with 1 μg/mL DAPI (Sigma-Aldrich) and washed three times and viewed on a fluorescence microscope (Carl Zeiss, Oberkochen, Germany).

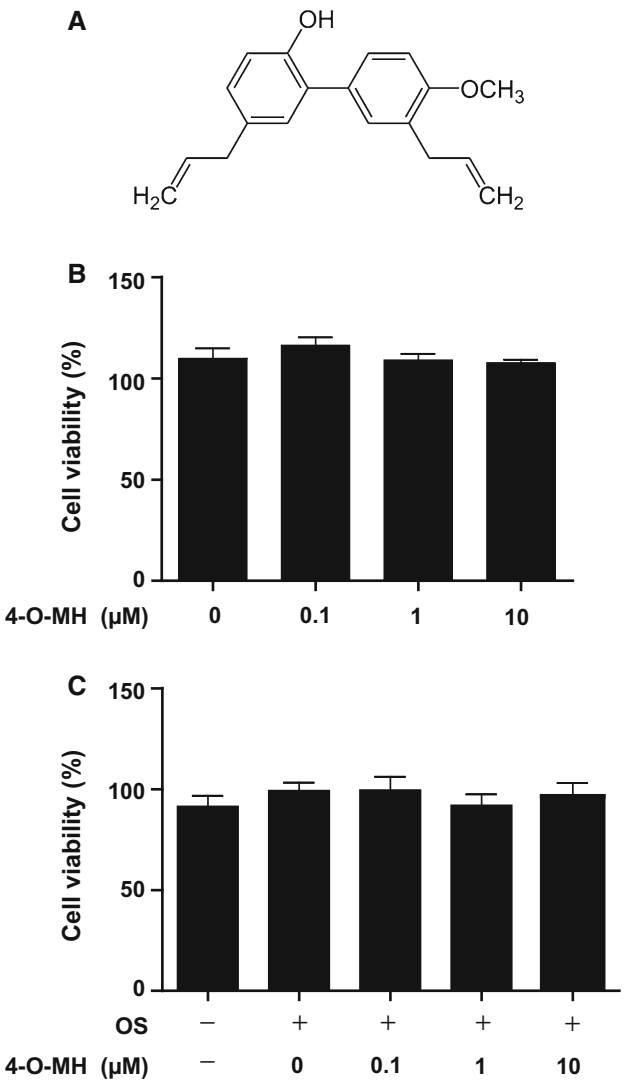

Fig. 1 Effects of 4-*O*-MH on cytotoxicity in primary mouse calvarial pre-osteoblasts. **a** Chemical structure of 4-*O*-methylhonokiol (4-*O*-MH). **b** After primary mouse calvarial pre-osteoblasts were seeded onto 96-well plates, 4-*O*-MH was added to cells at the indicated doses for 24 h. **c** Cells were cultured with 4-*O*-MH in osteogenic supplement medium (OS) containing 50 μg/mL L-ascorbic acid (L-AA) and 10 mM β-glycerophosphate (β-GP) for 5 days. Cell viability was measured using the MTT assay. Data are representative of three independent experiments

Western blot analysis

Cells were lysed and the protein concentration of lysates was determined using Bradford reagent (BioRad, Hercules, CA) as described previously (Yun et al. 2007). Equal amounts of lysate (20 μg) resolved by sodium dodecyl-polyacrylamide gel electrophoresis (SDS–PAGE) were transferred to a polyvinylidene fluoride (PVDF) membrane (Millipore, Bedford, MA), and the membrane was blocked with 1× TBS containing 0.05% Tween 20 (TBST) and 5% skim milk or 2% BSA for 1 h at room temperature. After blocking, the membranes were

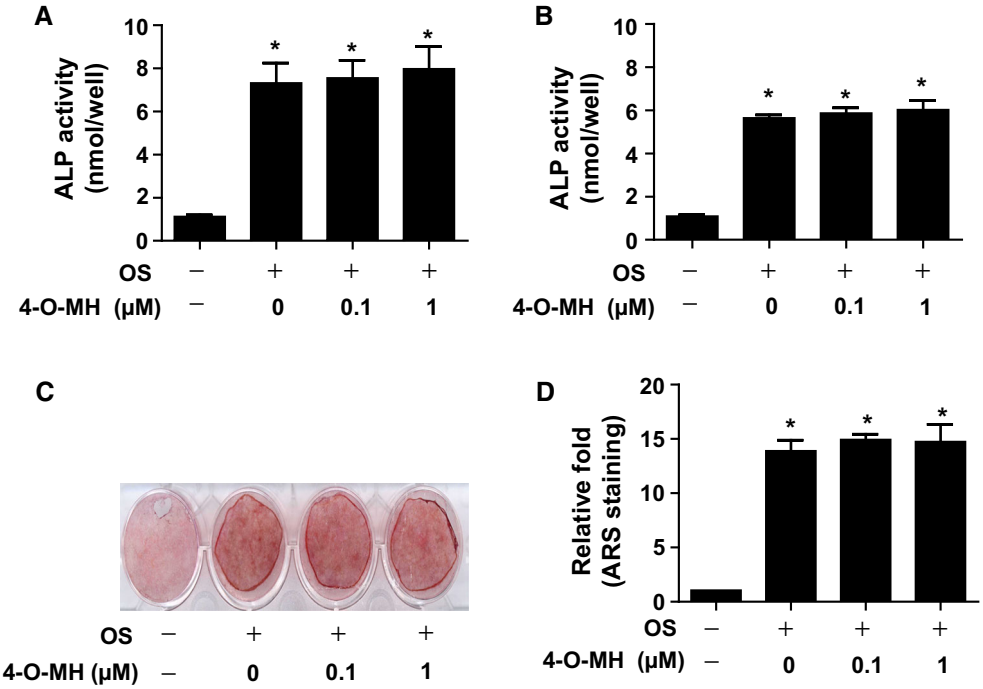

Fig. 2 Effects of 4-*O*-MH on osteoblast differentiation of primary mouse calvarial pre-osteoblasts. **a**, **b** Cells were seeded onto 48 well plates and cultured in OS containing 50 μg/mL L-AA and 10 mM β-GP with 4-*O*-MH (0, 0.1, and 1 μM) for 5 days (**a**) and 7 days (**b**). Alkaline phosphatase (ALP) activity was measured via ALP activity kit. **c, d** After cells were seeded onto 12 well plates, the cells were cultured in OS with 4-*O*-MH (0, 0.1, and 1 μM) for 14 days. Mineralized nodule formation was assessed by Alizarin red staining (C), and stains were eluted with DMSO to quantify the amount of alizarin red staining and measured at 590 nm. Data are represented as the relative fold of the control (**d**). *$p < 0.05$ compared to control. Data are representative of three independent experiments

incubated overnight at 4 °C with the respective primary antibodies. The membranes were washed with 1× TBST and incubated with diluted horseradish peroxidase (HRP)-conjugated secondary antibodies (1:10,000, Jackson ImmunoResearch, West Grove, PA) for 1 h at room temperature. After three washes, the membranes were detected using an enhanced chemiluminescence (ECL) kit (Millipore, Bedford, MA).

Quantitative real-time polymerase chain reaction (PCR) analysis

The total RNA of cells was extracted using TRIzol™ reagent (Life Technologies, Gaithersburg, MD) according to the manufacturer's instructions. RNA (1 μg) isolated from each sample was reverse-transcribed using oligo $(dT)_{15}$ primers with AccuPower® RT PreMix (iNtRON Biotechnology, Gyeonggi-do, South Korea). Next, the generated cDNAs were amplified with AccuPower® PCR PreMix (Bioneer Corporation, Daejeon, South Korea). For mRNA quantification, total RNA was extracted using the RNAqueous® kit and the cDNA was synthesized using 1 μg of total RNA with the High Capacity RNA-to-cDNA kit (Applied Biosystems, Foster City, CA) according to the manufacturer's protocol. Quantitative real-time PCR was performed using a LightCycler® 1.5 System (Roche Diagnostics GmbH, Mannheim, Germany). Thermocycling conditions consisted of an initial denaturation of 10 s at 95°C, followed by 45 cycles of 95°C for 10 s, 60°C for 5 s and 72°C for 10 s. For the calculation of relative quantification, the $2^{-\Delta\Delta C_T}$ formula was used, where $-\Delta\Delta C_T = (C_{T,target}–C_{T,\beta\text{-actin}})$ experimental sample—$(C_{T,target}–C_{T,\beta\text{-actin}})$ control sample.

Statistical analysis

The data were analyzed using GraphPad Prism version 5 software (GraphPad Software, Inc., San Diego, CA). Data are mean ± SEM. Statistical significance was evaluated using one-way analysis of variance (ANOVA) and the differences were assessed by the Dunnett's test. A value of $p < 0.05$ was considered to indicate statistical significance.

Results

4-*O*-MH has no cytotoxicity in primary mouse calvarial pre-osteoblasts and under osteoblast differentiation

To assess the cytotoxcity of 4-*O*-MH (Fig. 1a), cell viability was examined in primary mouse calvarial pre-

osteoblasts. Up to a concentration of 10 μM 4-*O*-MH, no cytotoxic effects were observed in the calvarial pre-osteoblasts (Fig. 1b) and under osteoblast differentiation in osteogenic supplement medium (OS) containing 50 μg/mL L-ascorbic acid (L-AA) and 10 mM β-glycerophosphate (β-GP) (Fig. 1c).

4-*O*-MH does not affect osteoblast differentiation of primary mouse calvarial pre-osteoblasts

Next, we investigated the effects of 4-*O*-MH on osteoblast differentiation in the presence or absence of 4-*O*-MH at non-cytotoxic concentrations (0.1–1 μM). First, the effect of 4-*O*-MH on osteoblast differentiation was carried out at 5 and 7 days by measuring the alkaline phosphatase (ALP) enzymatic activity as an early osteoblast differentiation marker. As shown in Fig. 2a and b, 4-*O*-MH did not affect ALP activity at concentrations ranging from 0.1 to 1 μM. Under the same conditions, the degree of mineralized nodule formation was determined at 14 days by using the ARS as a late osteoblast marker. Consistent with the effects on ALP activity, 4-*O*-MH also did not affect mineralized nodule formation (Fig. 2c). The quantification of mineralized nodule formation statistically validated the effect of 4-*O*-MH on osteoblast differentiation (Fig. 2d).

4-*O*-MH inhibits TRAP (+) MNCs and F-actin ring formation during RANKL-induced osteoclastogenesis

To examine the role of 4-*O*-MH in osteoclast differentiation, the cell toxicity of 4-O-MH was first determined in primary mouse BMMs derived from mouse whole bone marrow cells. The MTT assay showed no cytotoxic effects up to a concentration of 10 μM (Fig. 3a), and also showed no cytotoxic effects of 4-*O*-MH (0.1 and 1 μM) under osteoclast differentiation by 100 ng/mL RANKL (Fig. 3b). However, 4-*O*-MH suppressed osteoclast differentiation in a dose-dependent manner, as shown by a decrease in the TRAP-positive staining (Fig. 4a) and also a decrease in the proportion of TRAP-positive MNCs compared to the number of nuclei (Fig. 4b). Furthermore, 4-*O*-MH inhibited F-actin ring formation, a cytoskeletal structure that is essential for bone resorption in osteoclasts (Fig. 4c and d).

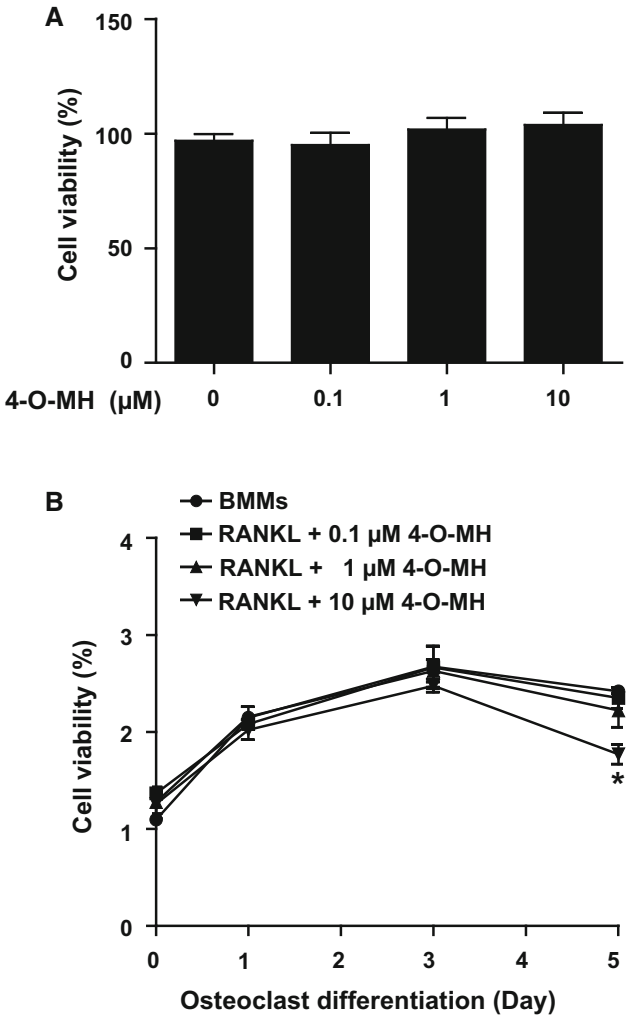

Fig. 3 Effects of 4-*O*-MH on cytotoxicity in primary mouse bone marrow macrophages. **a** After primary mouse bone marrow macrophages (BMMs) were seeded onto 96-well plates, 4-*O*-MH was added to cells at the indicated doses for 24 h. **b** The BMMs were cultured with 4-*O*-MH in 100 ng/mL RANKL for the indicated period. Cell viability was measured using the MTT assay. *$p < 0.05$ compared to the non-stimulated control group (BMMs). Data are representative of three independent experiments

4-*O*-MH inhibits osteoclast gene expression during RANKL-induced osteoclatogenesis

Next, we investigated the effects of 4-*O*-MH on mRNA expression for osteoclast differentiation and function. BMMs were differentiated for 3 days by 100 ng/mL RANKL in the presence or absence of 0.1–1 μM 4-*O*-MH. As shown in Fig. 5a–d, 4-*O*-MH downregulated gene expression of c-Fos and NF-ATc1 (initiation factor for osteoclast differentiation) as well as TRAP and integrin beta 3 (ITB3) (functional genes in osteoclasts).

4-*O*-MH inhibits RANKL-induced intracellular signaling pathways

To gain insight into the induction of osteoclast differentiation, we examined whether 4-*O*-MH influenced signaling pathways crucial for RANKL-induced osteoclastogenesis. Cells were treated with RANKL for 0, 5, 15, and 30 min in the presence or absence of 4-*O*-MH,

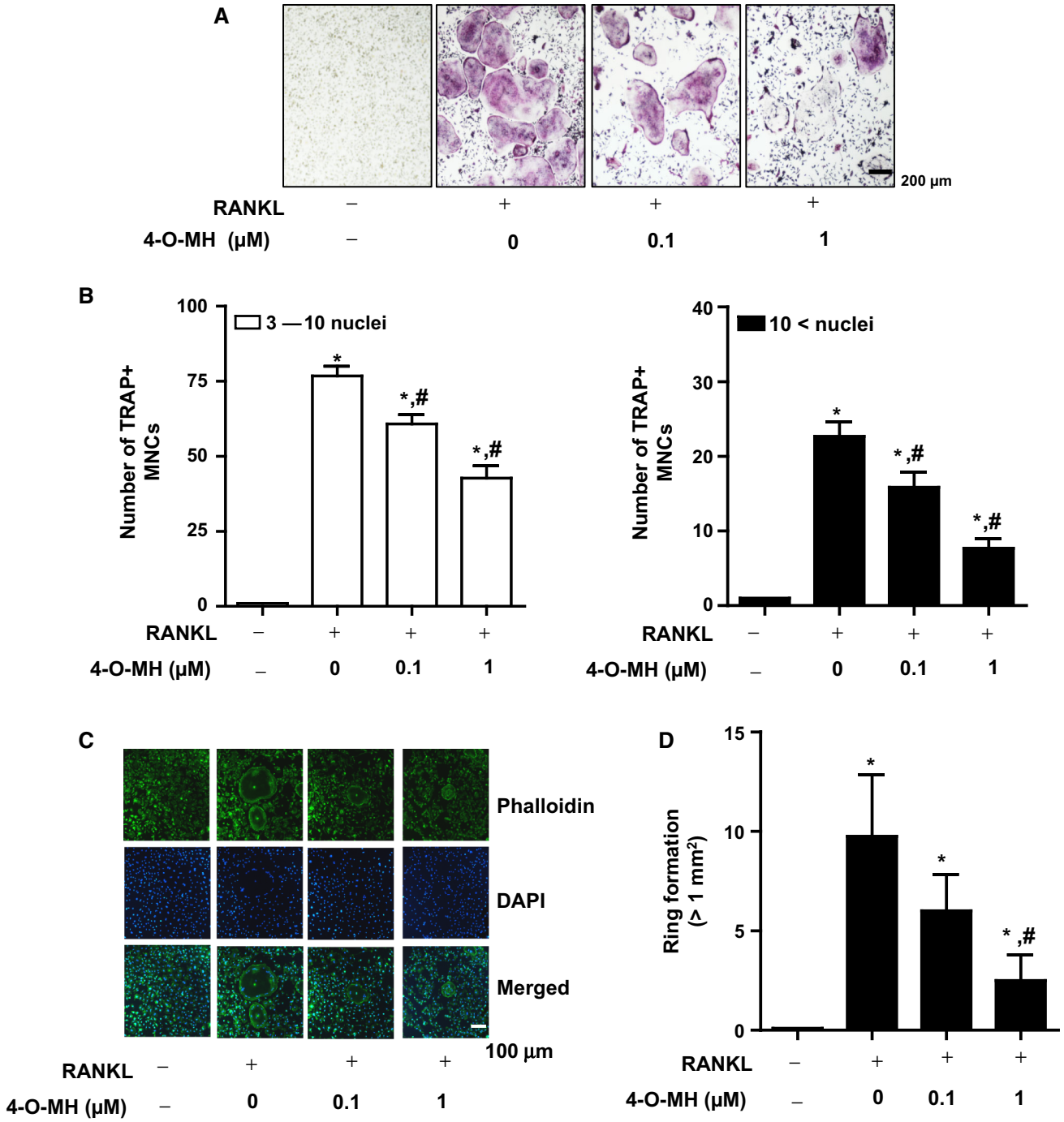

Fig. 4 Effects of 4-*O*-MH on RANKL-induced osteoclastogenesis in primary mouse bone marrow macrophages. **a**, **b** Bone marrow macrophages (BMMs) were seeded onto 48-well plates and cultured in 30 ng/mL M-CSF and 100 ng/mL RANKL with the indicated concentrations of 4-*O*-MH for 5 days. Mature osteoclasts were detected with TRAP staining (**a**). TRAP-positive MNCs and MNCs with more than three nuclei are shown. 0–10 nuclei (*left*), >10 nuclei (*right*) (**b**). *Scale bar* 200 μm. MNCs: multinucleated cells. **c, d** F-actin ring formation (*green*) was observed using a fluorescence microscope after staining with FITC-phalloidin (*green*) and DAPI (*blue*) (**c**), and then the number of rings formation (>1 mm^2) was measured (**d**). *Scale bar* 100 μm. *$p < 0.05$ compared to control. $^{\#}p < 0.05$ compared to RANKL. Data are representative of three independent experiments

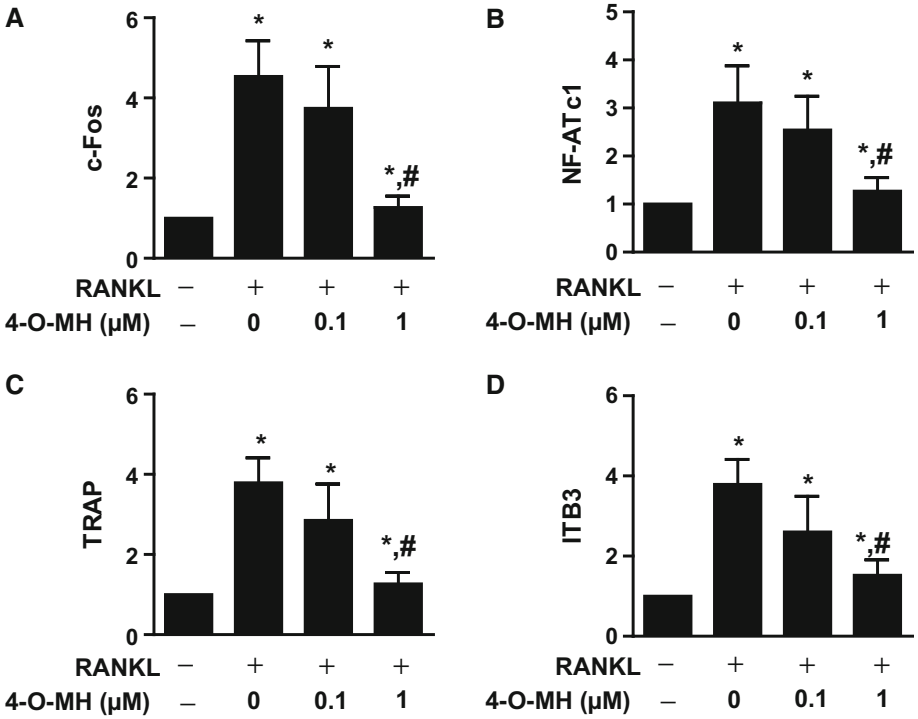

Fig. 5 Effects of 4-*O*-MH on osteoclast gene expression in RANKL-induced osteoclastogenesis. **a**–**d** Bone marrow macrophages (BMMs) were seeded onto 6-well plates and cultured in 30 ng/mL M-CSF and 100 ng/mL RANKL with the indicated concentrations of 4-*O*-MH for 3 days. Total RNA was isolated and osteoclast marker genes (c-Fos, NF-ATc1, TRAP, and ITB3) were analyzed by qRT-PCR. The values obtained for the target gene expression were normalized to β-actin and quantified relative to the expression in the non-stimulated control group. $^{*}p < 0.05$ compared to control. $^{\#}p < 0.05$ compared to RANKL. Data are representative of three independent experiments

and the activation of MAPKs (ERK1/2, p38, and JNK) was measured. Among them, the activation of ERK1/2 was specifically inhibited by 4-*O*-MH in a time dependent manner, as shown by a decrease in the phosphorylation of ERK1/2 (Fig. 6a). Additionally, RANKL-induced AKT and NF-κB signaling pathways were significantly attenuated by 4-*O*-MH (Fig. 6b, c).

Discussion

Osteoblast and osteoclast differentiation are a crucial aspect of bone formation and remodeling which is a process that is severely compromised in osteoporosis. For in vitro studies, calvarial pre-osteoblasts and BMMs isolated from calvaria and bone marrow were widely used for osteoblast and osteoclast differentiation, respectively (Chang et al. 2008; Yun et al. 2016). In the present study, we used primary mouse calvarial pre-osteoblasts and BMMs as an in vitro assay system for osteoblast and osteoclast differentiation. Natural compounds have been used to treat various diseases and investigated as a source for drug development (Lee et al. 2011c; Yun et al. 2014). In this study, we demonstrated that 4-*O*-MH isolated from *M. officinalis* did not affect osteoblast differentiation in calvarial pre-osteoblasts, whereas 4-*O*-MH displayed an inhibitory effect on RANKL-induced osteoclastogensis in BMMs.

Bone formation involves a complex series of events such as osteoblast differentiation and mineralized extracellular matrix formation by calcium deposition. ALP is a marker for early-stage osteoblast differentiation, and mineralized nodule formation is a phenotypic marker for late-stage differentiation (Lee et al. 2011a; Kim et al. 2014). Our results showed that 4-*O*-MH failed to modulate ALP activity and mineralized nodule formation in calvarial pre-osteoblasts. These data suggest that 4-*O*-MH does not have pharmacological properties in early and late osteoblastic differentiation, and in maturation.

Osteoclasts are large MNCs that are unique in their ability to resorb mineralized bone and are key players in physiological skeletal morphogenesis and bone remodeling (Teitelbaum and Ross 2003, 1996). Osteoclasts develop from monocyte-lineage hematopoietic precursors during a multistep differentiation process called osteoclastogenesis (Teitelbaum and Ross 2003, 1996). Osteoclasts form TRAP-positive MNCs and reorganize the actin cytoskeleton to attach to the bone surface, and then

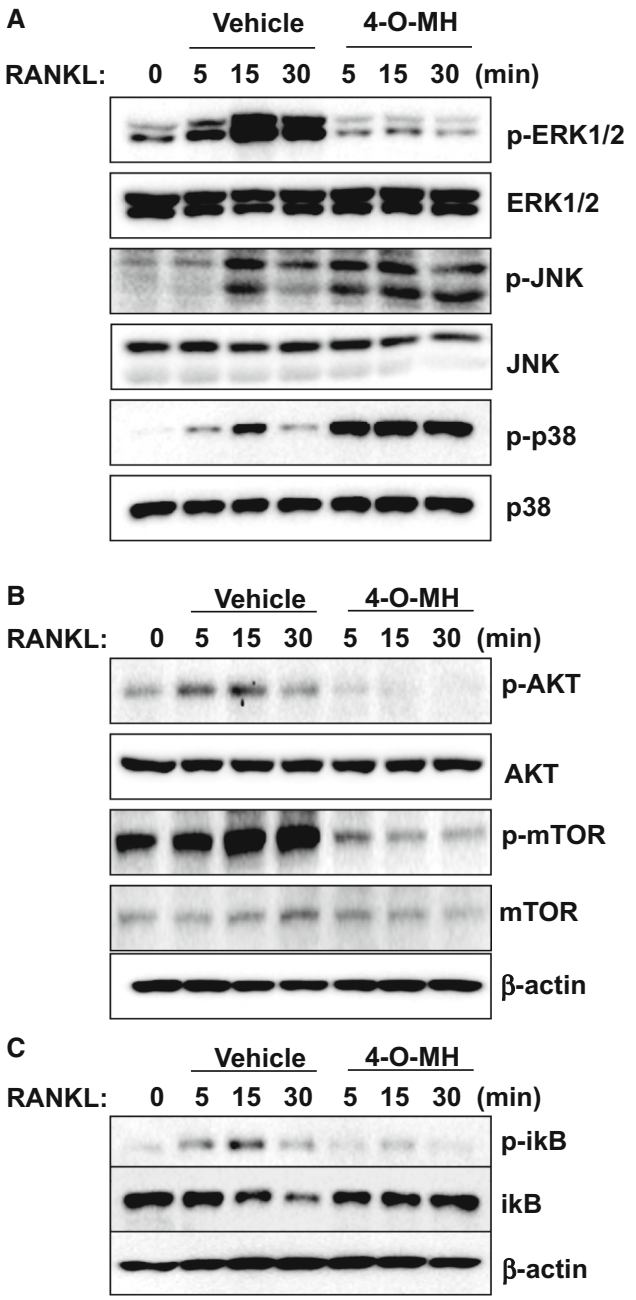

Fig. 6 Effects of 4-*O*-MH on RANKL-induced MAPKs, AKT, and NF-κB signaling pathways. **a**–**c** Cells were stimulated in 100 ng/mL RANKL with 4-*O*-MH for the indicated time. Equal amounts of lysate were analyzed by Western blotting and detected with antibodies against phospho-ERK (p-ERK), ERK, phospho-JNK (p-JNK), JNK, phospho-p38 (p-p38), and p38 for MAPKs signals (**a**), and antibodies against phospho-AKT (p-AKT), AKT, phospho-mTOR (p-mTOR), mTOR, and β-actin for AKT signals (**b**), and antibodies against IκB, phospho-IκB (p-IκB), and β-actin for NF-κB signals (**c**). Data are representative of three independent experiments

resorb the bone (Teitelbaum 2000; Boyle et al. 2003). In the present study, we demonstrated 4-O-MH suppressed the generation of TRAP-positive MNCs and F-actin ring formation by RANKL which belongs to the tumor necrosis factor TNF superfamily in BMMs. c-Fos, which is a major component of the transcription factor AP-1, is induced by RANKL, initiates osteoclast differentiation, and is responsible for the expression of another key regulator of osteoclastogenesis (Takayanagi et al. 2002; Takayanagi 2009; Kwak et al. 2010). In osteoclast precursors lacking c-Fos, NF-ATc1 is down-regulated, leading to impaired osteoclast differentiation and function (Matsuo et al. 2004). Our data also showed that 4-*O*-MH markedly downregulated the expression of c-Fos and NF-ATc1 (osteoclast differentiation genes) as well as TRAP and ITB3 (osteoclast-expressed genes). These data suggest that the RANKL-induced osteoclastogenesis is attenuated by 4-*O*-MH.

RANKL binds to its receptor RANK on osteoclast precursor cells and activates a variety of signaling pathways, including MAPK (ERK1/2, JNK, and p38 kinase), AKT, and NF-κB pathways, which can regulate transcription factors such as AP-1 and NF-ATc1, and proteins such as TRAP and ITB3 (Whitmarsh and Davis 1996; Monje et al. 2005). Our results showed that 4-*O*-MH reduced RANK-induced ERK1/2 as well as AKT and NF-κB pathways. Interestingly, 4-*O*-MH potentiated RANK-induced JNK and p38 pathways. In the future, other possible roles for 4-*O*-MH in ERK1/2, JNK, and p38 pathways under RANKL-induced osteoclastogenesis will be investigated. Taken together, we suggest that 4-*O*-MH suppresses osteoclast differentiation and function through RANKL-induced ERK1/2, AKT, and NF-κB pathways together with osteoclast gene expression.

In conclusion, this study is the first report for possible roles of 4-*O*-MH in primary cultures of mouse calvarial pre-osteoblasts and BMMs. We found that 4-*O*-MH specifically inhibits RANKL-induced osteoclastogenesis in bone-forming cells and bone-resorbing cells. Although the present study demonstrates the anti-osteoclastogenic potency and related mechanisms of 4-*O*-MH, further investigation is necessary to understand its benefit in animals. The mechanism of action that underlies the effects of 4-*O*-MH on RANKL-induced osteoclastogenesis is shown in Fig. 7. Together, our findings suggest that 4-*O*-MH may be an effective anabolic agent in bone-destructive diseases such as osteoporosis, periodontal disease, and osteoarthritis.

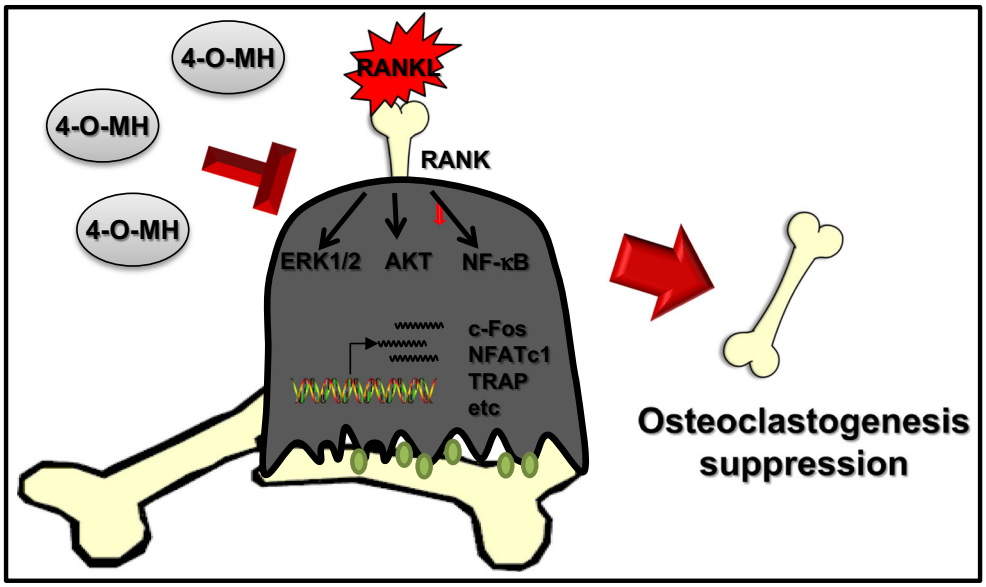

Fig. 7 Schematic diagrams for osteoclastogenesis modulation by 4-*O*-MH. When RANKL binds RANK on bone marrow macrophages (BMMs), osteoclastogenesis is initiated. However, pretreatment of 4-*O*-MH suppresses RANKL-induced osteoclastogenesis via inactivation of downstream signaling pathways and downregulation of osteoclast gene expression

Acknowledgements This work was supported by a grant from Kyung Hee University in 2016 (KHU-20160546) and the National Research Foundation of Korea (NRF) grant funded by the Korea government (MEST) (MRC, 20080062275; 2015R1D1A1A01059240).

Compliance with ethical standards

Conflict of interest The authors declare that they have no competing financial interests.

References

Boyle WJ, Simonet WS, Lacey DL (2003) Osteoclast differentiation and activation. Nature 423:337–342

Cairoli E, Zhukouskaya VV, Eller-Vainicher C, Chiodini I (2015) Perspectives on osteoporosis therapies. J Endocrinol Invest 38:303–311

Chang EJ, Ha J, Oerlemans F, Lee YJ, Lee SW, Ryu J, Kim HJ, Lee Y, Kim HM, Choi JY, Kim JY, Shin CS, Pak YK, Tanaka S, Wieringa B, Lee ZH, Kim HH (2008) Brain-type creatine kinase has a crucial role in osteoclast-mediated bone resorption. Nat Med 14:966–972

Endo I, Matsumoto T (2012) Update and perspectives of anabolic therapies for osteoporosis. Clin Calcium 22:327–333

Filvaroff E, Erlebacher A, Ye J, Gitelman SE, Lotz J, Heillman M, Derynck R (1999) Inhibition of TGF-beta receptor signaling in osteoblasts leads to decreased bone remodeling and increased trabecular bone mass. Development 126:4267–4279

Jung YY, Lee YJ, Choi DY, Hong JT (2014) Amelioration of cognitive dysfunction in APP/PS1 double transgenic mice by long-term treatment of 4-*O*-methylhonokiol. Biomol Ther (Seoul) 22:232–238

Khosla S, Riggs BL (2005) Pathophysiology of age-related bone loss and osteoporosis. Endocrinol Metab Clin North Am 34:1015–1030

Kim MB, Song Y, Hwang JK (2014) Kirenol stimulates osteoblast differentiation through activation of the BMP and Wnt/beta-catenin signaling pathways in MC3T3-E1 cells. Fitoterapia 98:59–65

Kwak HB, Lee BK, Oh J, Yeon JT, Choi SW, Cho HJ, Lee MS, Kim JJ, Bae JM, Kim SH, Kim HS (2010) Inhibition of osteoclast differentiation and bone resorption by rotenone, through down-regulation of RANKL-induced c-Fos and NFATc1 expression. Bone 46:724–731

Lee HS, Jung EY, Bae SH, Kwon KH, Kim JM, Suh HJ (2011a) Stimulation of osteoblastic differentiation and mineralization in MC3T3-E1 cells by yeast hydrolysate. Phytother Res 25:716–723

Lee YJ, Choi IS, Park MH, Lee YM, Song JK, Kim YH, Kim KH, Hwang DY, Jeong JH, Yun YP, Oh KW, Jung JK, Han SB, Hong JT (2011b) 4-*O*-methylhonokiol attenuates memory impairment in presenilin 2 mutant mice through reduction of oxidative damage and inactivation of astrocytes and the ERK pathway. Free Radic Biol Med 50:66–77

Lee YJ, Lee YM, Lee CK, Jung JK, Han SB, Hong JT (2011c) Therapeutic applications of compounds in the *Magnolia* family. Pharmacol Ther 130:157–176

Lee YJ, Choi DY, Choi IS, Kim KH, Kim YH, Kim HM, Lee K, Cho WG, Jung JK, Han SB, Han JY, Nam SY, Yun YW, Jeong JH, Oh KW, Hong JT (2012) Inhibitory effect of 4-*O*-methylhonokiol on lipopolysaccharide-induced neuroinflammation, amyloidogenesis and memory impairment via inhibition of nuclear factor-kappaB in vitro and in vivo models. J Neuroinflammation 9:35

Marie PJ, Kassem M (2011) Osteoblasts in osteoporosis: past, emerging, and future anabolic targets. Eur J Endocrinol 165:1–10

Matsuo K, Galson DL, Zhao C, Peng L, Laplace C, Wang KZ, Bachler MA, Amano H, Aburatani H, Ishikawa H, Wagner EF (2004) Nuclear factor of activated T-cells (NFAT) rescues osteoclastogenesis in precursors lacking c-Fos. J Biol Chem 279:26475–26480

Monje P, Hernandez-Losa J, Lyons RJ, Castellone MD, Gutkind JS (2005) Regulation of the transcriptional activity of c-Fos by ERK. A novel role for the prolyl isomerase PIN1. J Biol Chem 280:35081–35084

Oh JH, Kang LL, Ban JO, Kim YH, Kim KH, Han SB, Hong JT (2009) Anti-inflammatory effect of 4-*O*-methylhonokiol, compound isolated from *Magnolia officinalis* through inhibition of NF-kappaB. Chem Biol Interact 180:506–514

Oh JH, Ban JO, Cho MC, Jo M, Jung JK, Ahn B, Yoon DY, Han SB, Hong JT (2012) 4-*O*-methylhonokiol inhibits colon tumor growth via p21-mediated suppression of NF-kappaB activity. J Nutr Biochem 23:706–715

Riggs BL, Hartmann LC (2003) Selective estrogen-receptor modulators—mechanisms of action and application to clinical practice. N Engl J Med 348:618–629

Riggs BL, Parfitt AM (2005) Drugs used to treat osteoporosis: the critical need for a uniform nomenclature based on their action on bone remodeling. J Bone Miner Res 20:177–184

Takayanagi H (2009) Osteoimmunology and the effects of the immune system on bone. Nat Rev Rheumatol 5:667–676

Takayanagi H, Kim S, Koga T, Nishina H, Isshiki M, Yoshida H, Saiura A, Isobe M, Yokochi T, Inoue J, Wagner EF, Mak TW, Kodama T, Taniguchi T (2002) Induction and activation of the transcription factor NFATc1 (NFAT2) integrate RANKL signaling in terminal differentiation of osteoclasts. Dev Cell 3:889–901

Teitelbaum SL (2000) Bone resorption by osteoclasts. Science 289:1504–1508

Teitelbaum SL, Ross FP (2003) Genetic regulation of osteoclast development and function. Nat Rev Genet 4:638–649

Vondracek SF, Minne P, McDermott MT (2008) Clinical challenges in the management of osteoporosis. Clin Interv Aging 3:315–329

Whitmarsh AJ, Davis RJ (1996) Transcription factor AP-1 regulation by mitogen-activated protein kinase signal transduction pathways. J Mol Med (Berl) 74:589–607

Yun HM, Kim S, Kim HJ, Kostenis E, Kim JI, Seong JY, Baik JH, Rhim H (2007) The novel cellular mechanism of human 5-HT6 receptor through an interaction with Fyn. J Biol Chem 282:5496–5505

Yun HM, Ban JO, Park KR, Lee CK, Jeong HS, Han SB, Hong JT (2014) Potential therapeutic effects of functionally active compounds isolated from garlic. Pharmacol Ther 142:183–195

Yun HM, Park KR, Quang TH, Oh H, Hong JT, Kim YC, Kim EC (2015) 2,4,5-Trimethoxyldalbergiquinol promotes osteoblastic differentiation and mineralization via the BMP and Wnt/beta-catenin pathway. Cell Death Dis 6:e1819

Yun HM, Park KR, Hong JT, Kim EC (2016) Peripheral serotonin-mediated system suppresses bone development and regeneration via serotonin 6 G-protein-coupled receptor. Sci Rep 6:30985

Zanotti S, Canalis E (2015) Activation of Nfatc2 in Osteoblasts Causes Osteopenia. J Cell Physiol 230:1689–1695